

CE-based white-box adversarial attacks will not work using super-fitting

Youhuan Yang^{1,2}, Lei Sun (✉)², Leyu Dai², Song Guo², Xiuqing Mao², Xiaoqin Wang², Bayi Xu^{1,2}

¹ School of Cyber Science and Engineering, Zhengzhou University, Zhengzhou 450000, China

² Information Engineering University, Zhengzhou 450001, China

Abstract Deep neural networks are widely used in various fields because of their powerful performance. However, recent studies have shown that deep learning models are vulnerable to adversarial attacks, i.e., adding a slight perturbation to the input will make the model obtain wrong results. This is especially dangerous for some systems with high-security requirements, so this paper proposes a new defense method by using the model super-fitting state to improve the model’s adversarial robustness (i.e., the accuracy under adversarial attacks). This paper mathematically proves the effectiveness of super-fitting and enables the model to reach this state quickly by minimizing unrelated category scores (MUCS). Theoretically, super-fitting can resist any existing (even future) CE-based white-box adversarial attacks. In addition, this paper uses a variety of powerful attack algorithms to evaluate the adversarial robustness of super-fitting, and the proposed method is compared with nearly 50 defense models from recent conferences. The experimental results show that the super-fitting method in this paper can make the trained model obtain the highest adversarial robustness.

Keywords adversarial attack, white-box, super-fitting.

1 Introduction

Many studies have shown that the deep learning models [1–4] widely used in various fields are very fragile. Attackers could fool the classifier to achieve evasion attacks by adding slight perturbations to the original examples (adversarial examples) that are difficult to distinguish by human eyes. Meanwhile, various types of defense algorithms with different capabilities (adversarial robustness) have been proposed. Though these algorithms can well handle existing attack methods, they cannot achieve the same effect on future attack methods. Image preprocessing [5, 6] and defensive distillation [7] do not depend on adversarial examples. These algorithms are effective for various attack methods, but their performance is suboptimal. Adversarial training [8] is considered the most effective defense method at present (many methods are based on adversarial training), and these algorithms rely on adversarial examples (or specific types of adversarial attack algorithms). The existing adversarial defense methods share some shortcomings: 1) the adversarial robustness (accuracy) is too low, i.e., the performance of the defense model on adversarial examples is much lower than that on the original clean examples; 2) the generalization against unknown attacks is poor, and these algorithms often cannot defense effectively when a more advanced (or future) attack algorithm is proposed; 3) the implementation is complicated, and most of these defense

methods have too many hyperparameters. Also, the hyperparameters of the training process requires careful tuning. Therefore, it is acknowledged that adversarial defense is a very difficult task.

Since Szegedy et al. [9] first discovered the existence of adversarial examples, various studies on adversarial attack algorithms have developed rapidly. However, most of these attack algorithms (including white- and black-box attacks) are based on Cross-Entropy (CE) loss, and only a few attack algorithms use other (or self-define) loss functions (such as AutoAttack [10], C&W [11], etc.). This paper proposes a new defense method based on super-fitting for these widely CE-based white-box adversarial attacks. Super-fitting is a state of model training. In this state, the gradient information calculated by the CE loss will die out (i.e., Gradient Vanishing). In the experiment, it is found that the model in this state defense against almost any CE-based white-box adversarial attacks in existence. In the subsequent introductions, this paper explains the reason for this phenomenon and the mathematical principle of defense and proposes a method called MUCS to enable the defense model to quickly reach the super-fitting state. The contributions of this paper are as follows:

- This paper proposes the concept of super-fitting in the model training phase. In this state, the model can defend almost all existing CE-based white-box adversarial attacks, and the training phase is not related to the adversarial attack algorithm. Through analysis, it can be seen that the model trained using the super-fitting method can defend against future CE-based white-box adversarial attacks.
- This paper analyzes the reason for the super-fitting phenomenon and proposes the MUCS method to reduce the number of model training iterations to reach this state, which makes it easy to train a super-fitting model without high-power graphics.
- Finally, this paper experimentally proves the effectiveness of the proposed method. Compared with nearly 50 defense models from top conferences (e.g., ICML, NeurIPS, ICLR, ICCV, CVPR). The experimental results indicate that super-fitting obtains the highest adversarial robustness against CE-based white-box adversarial attacks.

2 Preliminaries

2.1 Adversarial attack

Although deep neural networks perform well in many fields (e.g., face recognition, object detection, medical image pro-

cess, malicious traffic detection, etc.), many studies [8, 12–14] show that deep neural networks are very fragile and vulnerable to adversarial attacks, i.e., adding slight perturbations to the input that are hard to distinguish with the human eyes (adversarial perturbations) will make the classifier obtain unexpected results. The constrained optimization problem is defined as:

$$\begin{aligned} y \neq \arg \max f(x + \delta) \\ \text{s.t. } \|\delta\|_p \leq \epsilon \end{aligned} \quad (1)$$

In Eq. (1), $\|\bullet\|_p$ denotes L - p norm. $p \in \{1, 2, \infty\}$, and this paper sets $p = \infty$, i.e., just considers $L - \infty$ attack; ϵ is a hyperparameter that limits the size of adversarial perturbations; x and $x + \delta \in [0, 1]^D$ denote origin images and adversarial images, respectively; $\delta \in [-\epsilon, +\epsilon]^D$ denote perturbations; x is the input of classifier f , and y is the true label. Goodfellow et al. [12] proposed the Fast Gradient Sign Method (FGSM) based on the definition of adversarial attacks in Eq. (1). An adversarial attack could be formulated as follows:

$$x_{adv} = x + \epsilon \text{sign}(\nabla_x \mathcal{L}(f(x), y)) \quad (2)$$

In Eq. (2), sign represents the sign function, \mathcal{L} is the loss function (i.e., CE loss in this paper), and x_{adv} is the adversarial example generated by the adversarial attack algorithm. Based on FGSM, Kurakin et al. [13] proposed a stronger multi-step iterative attack algorithm called Basic Iterative Method (BIM), which uses a smaller step size in each gradient ascent iteration process (attack process). Similar to the BIM algorithm, Madry et al. [8] found that adding random noise to the input during the restart phase of the attack algorithm can make it stronger (i.e., approaching the lower bound of robustness). Projected Gradient Descent (PGD) generates an adversarial example by performing the iterative update:

$$x_{adv}^{t+1} = \text{Proj}_{(x,\epsilon)}(x_{adv}^t + \alpha \text{sign}(\nabla_{x_{adv}^t} \mathcal{L}(f(x_{adv}^t), y))) \quad (3)$$

where,

$$\begin{aligned} x_{adv}^0 &= x_{orig} + \delta_0 \\ \text{s.t. } \|\delta_0\|_\infty &\leq \epsilon \end{aligned}$$

In Eq. (3), t is the number of iterations, x_{orig} is the original image, δ_0 is the randomly initialized noise, $\text{Proj}_{(x,\epsilon)}$ is the operation to clip perturbations in ϵ -ball constrain, and α is the step size of every single attack. Many researchers have made improvements to PGD. For example, Croce et al. [10] proposed Adaptive Projected Gradient Descent (APGD). Unlike the original PGD, APGD does not have a fixed step size,

i.e., α will dynamically change in each iteration according to the value of the loss function.

Obtaining an attack starting point x_{adv}^0 by random initialization is always suboptimal (e.g., ODI [15] and AutoAttack [10]). So, Liu et al. [16] proposed Adaptive Auto Attack (A^3), which is quite different from PGD in starting point initialization. To be specific, given a random direction of diversification w_d sampled from uniform distributions $U(-1, 1)^K$ (K is the total number of categories for the classification task), A^3 firstly calculates a normalized perturbation vector as follows:

$$v(x, f, w_d) = \frac{\nabla_x w_d^T f(x)}{\|\nabla_x w_d^T f(x)\|} \quad (4)$$

Then, the starting point is calculated through the following iterative process:

$$x_{init}^{t+1} = P_{(x,\epsilon)}(x_{init}^t + \alpha_{init} \text{sign}(v(x_{init}^t, f, w_d))) \quad (5)$$

When the T -th initialization iteration ends, $x_{adv}^0 = x_{init}^T$ is selected as the attack starting point, and then A^3 chooses an attack process similar to PGD. Differently, its step size is not fixed compared to PGD. The step size of the n -th round of attack (assuming a total of N rounds of iterative attacks) is calculated as follows:

$$\alpha^n = \frac{1}{2} \epsilon \bullet (1 + \cos(\frac{n \bmod N}{N} \pi)) \quad (6)$$

It is worth noting that the original A^3 uses the statistical results to modify the distribution information of the w_d part of the dimension after randomly obtaining w_d . The subsequent experimental part of this paper does not take this approach. This is because the increase in revenue is small. Also, the original A^3 uses Margin loss for attacks, but this paper uses the CE loss.

It can be seen that in general, the white-box attack is based on the gradient, and most attack methods use the CE loss when calculating the gradient information to attack the classifier. The main reason is that the current classification tasks generally use the CE loss for model training. Its calculation formula is as follows:

$$\mathcal{L}(z, y) = -z_y + \ln\left(\sum_{i=0}^{K-1} e^{z_i}\right) \quad (7)$$

In Eq. (7), z is the output of the classifier (logits vector, $z \in \mathbb{R}^K$), and y is the true label of the example ($y \in [0, K)$). Although CE loss is the most popular loss function to obtain gradients for adversarial attacks, its shortcomings are also obvious. When $z_k \rightarrow -\infty$ ($k \in [0, K)$, $k \neq y$), there will be a *Gradient Vanishing* situation. The specific explanation and formulation will be presented in Section 3.

2.2 Adversarial defense

To address the adversarial attack threat, different types of defense algorithms have been proposed, e.g., image pre-processing [5, 6], adversarial training [8], gradient obfuscation/hiding [17], regularization [18, 19], etc. Among them, adversarial training is currently considered to be the most effective defense method, and its optimization process is defined as follows:

$$\min_{\theta} E_{(x,y)^D} \max_{\|\delta\|_p \leq \epsilon} \mathcal{L}(\theta, f(x + \delta), y) \quad (8)$$

Eq. (8) contains two optimization problems, namely the inner maximization and outer minimization problems. The inner maximization problem always tries to find the worst-case examples (adversarial examples), and the outer minimization problem is to train a model robust to adversarial examples. Many studies are based on the above-mentioned standard adversarial training. For example, CAT [20] uses a small number of iterations in the initial stage of model training, and it increases the number of iterations of the attack when the model achieves a high accuracy against the current attack. FAT [21] adopts early stopping in the inner maximization problem to approach the lower robustness boundary. In addition to this, there is a part of work dedicated to reducing the time of adversarial training, e.g., YOPO [22], FAST-AT, [23], etc. For example, TRADES [18] attempts to balance accuracy between clean examples and adversarial examples. There are many methods based on adversarial training, and the performance gap between these methods is not large. A common point of view is the improvement of robustness largely depends on the internal maximization problem. A stronger attack algorithm will make the defense model more robust, but the cost will also be greater.

Different from adversarial training, defensive distillation [7] is a gradient hiding method, which uses real labels (hard labels) to train the teacher network and uses the output of the teacher network as the soft label of the student network. The calculation of the softmax function with temperature (used to calculate the loss value) is defined as:

$$F(z, y, T) = \frac{e^{z_i/T}}{\sum_{i=0}^{K-1} e^{z_i/T}} \quad (9)$$

Particularly, Eq. (9) is a normal softmax function when $T = 1$. It can be seen that although defensive distillation can hide the gradient information of the teacher network to a certain extent, gradient information will still be leaked through the student network.

Although various defense methods have been proposed to resist adversarial attacks, the results are unsatisfactory, and

there is no effective method that can make the defense model achieve a similar accuracy on adversarial examples to that on clean examples. Most importantly, current defense methods cannot defend well both mathematically and experimentally, even in the face of CE-based adversarial attacks that have existed for a long time.

3 Super-fitting

In this section, the super-fitting phenomenon in the model training phase and its explanation are first introduced. Then, the method MUCS is proposed to accelerate the model to reach the super-fitting state.

3.1 Phenomenon

The general model training state changes from under-fitting (at the beginning of the training phase) to fitting (the training is completed) and finally reaches the state of over-fitting. Since over-fitting will reduce the generalization of the trained model, researchers always choose to stop training when the model reaches the fitting state during the training process. However, through an experiment, this paper found that the concepts of different fitting states are relative, and over-fitting on the original/clean examples is under-fitting on the adversarial examples. By increasing the number of iterations of the training phase, the model can also reach the state of fitting on adversarial examples. This state is far behind over-fitting for clean examples, which is called super-fitting in this paper. This paper uses MiddleCNN (the network consists of three convolutional layers with 64, 128 and 256 output channels, respectively, and two fully connected layers with 1024 and 10 units, respectively. Each convolutional layer is followed by BatchNormalization [24], LeakReLU and Maxpooling layer.) and ResNet-18 [1] to train defense models on the CIFAR-10 dataset to make them super-fitting. Fig. 1 shows the partial information of the two defense models in the training phase (top MiddleCNN, bottom ResNet-18), including the accuracy of clean examples for the training set and the accuracy of adversarial examples for the test set (left) and the value of the loss function (right) calculated on adversarial examples using the CE loss.

In the experiment, both models are trained using clean examples, the CE loss, and the Adam [25] optimizer (the learning rate is set to 1e-3, and other parameters used in the training process are set to the default). No defensive measures are used, and just the number of training iterations is increased (max epoch is 30000). Afterward, PGD-20 ($\epsilon = 8.0/255$,

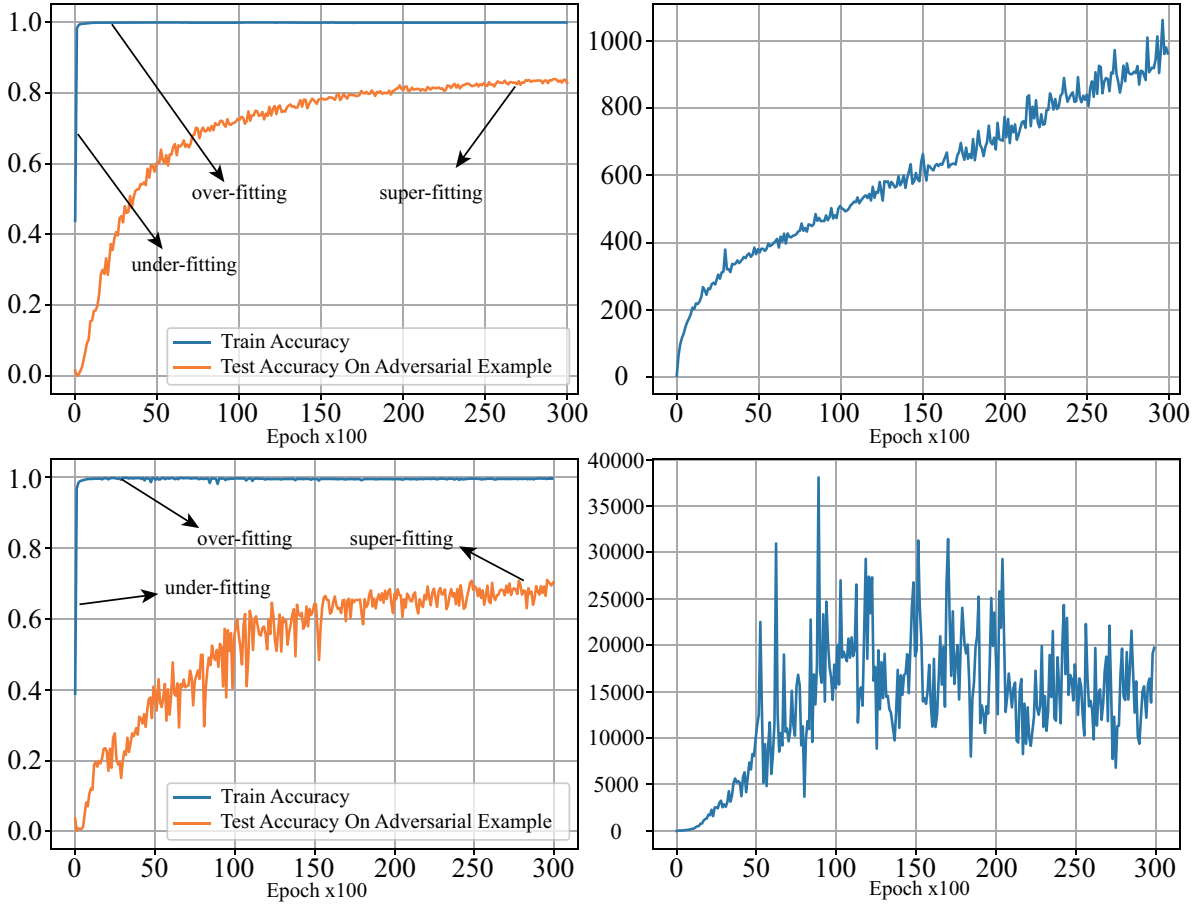


Fig. 1: Different fitting states on CIFAR-10

step size is $\epsilon/10$) is used on the CIFAR-10 test set to evaluate the accuracy. The accuracy of MiddleCNN on the adversarial examples generated by PGD-20 is 83.72% (the accuracy on clean examples is 88.97%), and the adversarial robustness of ResNet-18 is 68.75% (the accuracy on clean examples is 83.85%).

Obviously, super-fitting only sacrifices a part of generalization (the accuracy on the clean examples is lower than that in the fitting state), but it greatly improves the adversarial robustness of the model. Surprisingly, the loss function value of the adversarial examples calculated with the CE loss in Fig. 1 is increasing (theoretically it should be a very small value). To find the reason for this phenomenon, this paper shows the statistics of the prediction results (logits) of each category of CIFAR-10 by MiddleCNN in the super-fitting state in Fig. 2.

In Fig. 2, the output information of the same categories of examples is in the same subplot. There are 10 bars in each subplot, and the values are the mean of model output in each dimension on the category of examples, i.e., the prediction

scores of each category given by the model. It can be seen from the figure that the prediction scores of the examples in the super-fitting state of the MiddleCNN are polarized. The predicted values of examples in the dimension of the real label are much larger than others, and the values in the dimensions that do not belong to the real label are generally much smaller than 0.

Inspired by the distribution of the example output results in Fig. 2, this paper analyzes the impact of logits changes on the CE loss. It is found that when the model outputs meet $z_k \rightarrow -\infty$ ($k \in [0, K]$ and $k \neq y$), the CE-based white-box adversarial attack algorithm will not work.

3.2 Analysis

Since $\ln x$ cannot be differentiated when $x \leq 0$, the CE loss shown in Eq. (7) often adopts an equivalent calculation:

$$\mathcal{L}(b, t) = - \sum_{i=0}^{K-1} t_i b_i \quad (10)$$

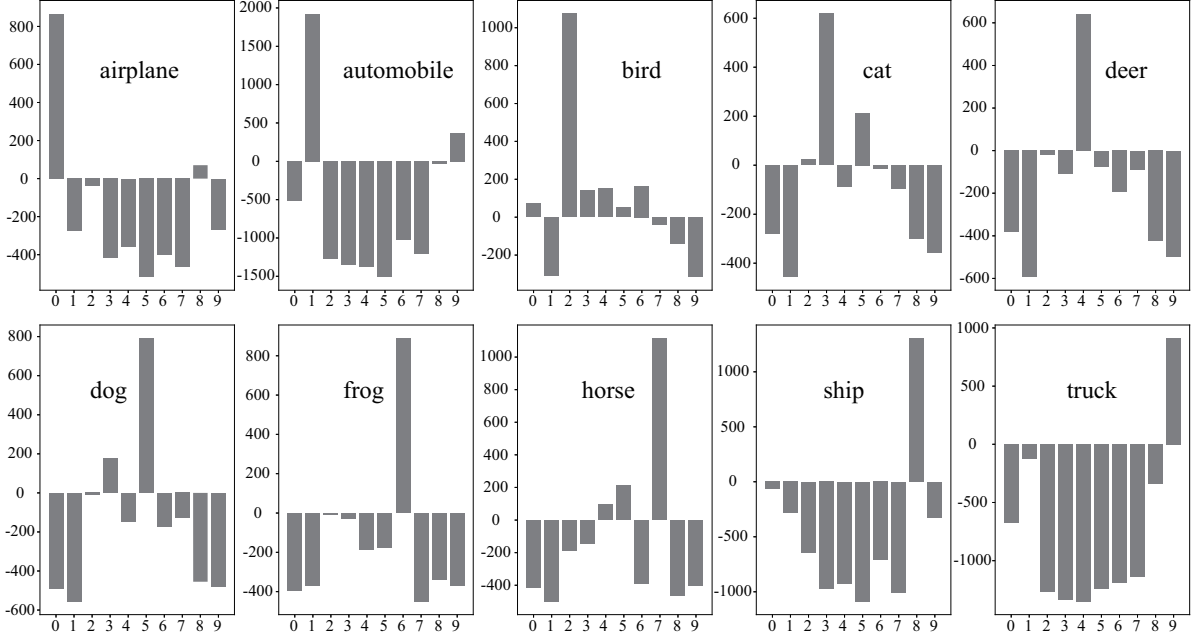


Fig. 2: Logits statistics for each category

where,

$$t_i = \begin{cases} 1 & i = y \\ 0 & \text{others} \end{cases}$$

$$b_i = \ln \frac{e^{z_i}}{\sum_{j=0}^{K-1} e^{z_j}} = z_i - \ln \sum_{j=0}^{K-1} e^{z_j} \quad (11)$$

b is the result of the model output after passing through the softmax and \ln functions; t is the one-hot encoding format of the true label of the example. From Eq. (10) and Eq. (11), it can be deduced:

$$\frac{\partial \mathcal{L}}{\partial b_i} = -t_i = \begin{cases} -1 & i = y \\ 0 & \text{others} \end{cases} \quad (12)$$

$$\frac{\partial \mathcal{L}}{\partial z_i} = \sum_{j=0}^{K-1} \frac{\partial \mathcal{L}}{\partial b_j} \frac{\partial b_j}{\partial z_i} = \frac{\partial \mathcal{L}}{\partial b_y} \frac{\partial b_y}{\partial z_i} = -\frac{\partial b_y}{\partial z_i} \quad (13)$$

$$b_y = z_y - \ln \sum_{j=0}^{K-1} e^{z_j} \quad (14)$$

Then,

$$\frac{\partial \mathcal{L}}{\partial z_i} = \begin{cases} \frac{e^{z_y}}{\sum_{j=0}^{K-1} e^{z_j}} - 1 & i = y \\ \frac{e^{z_i}}{\sum_{j=0}^{K-1} e^{z_j}} & \text{others} \end{cases} \quad (15)$$

It is easy to find $e^{z_k} \rightarrow 0$ when $z_k \rightarrow -\infty$ ($k \in [0, K)$ and $k \neq y$). Then,

$$\frac{\partial \mathcal{L}}{\partial z_i} = 0 \quad (16)$$

There will be a gradient vanishing at this time, i.e., the CE-based white-box adversarial attack will not work because the

gradient information cannot be propagated. Therefore, this paper mathematically explains how super-fitting resists adversarial attacks. Based on this, the method proposed in this paper can defend against future CE-based white-box adversarial attacks.

However, super-fitting will face two problems: 1) z_k cannot reach the mathematical $-\infty$; 2) cost too much time (ResNet-18 needs about 30,000 iterations or a few days to reach the super-fitting state even with an RTX3090 graphics card). Under the floating-point operation of modern computers, the first problem can be solved easily by optimizing z_k to a very small value ($z_k < 0$, it does not need to reach the mathematical $-\infty$). In this case, e^{z_k} will be zero, and Eq. (16) holds. To solve the second problem, a new optimization process is proposed in this paper to minimize unrelated category scores, and the specific implementation is introduced in Section 3.3.

3.3 MUCS: Minimize unrelated category scores

Although training the model with the CE loss can also make it super-fitting, the process consumes a lot of time. Also, it is difficult to achieve a perfect super-fitting state (e.g., experiment in Fig. 1) when the model parameters are large (e.g., ResNet-18). To address these issues, this paper proposes a new optimization method called MUCS, and the new optimization problem is defined as:

$$\text{minimize } (z_s - z_y) \quad (17)$$

Table 1: Performance of MUCS compare to the CE loss

Model		Iterations	Clean Accuracy	Robustness Accuracy
MiddleCNN	CE-Loss	30,000	88.97%	83.45%
	MUCS	500	86.86%	85.83%
ResNet-18	CE-Loss	30,000	84.10%	69.72%
	MUCS	3,000	82.65%	84.21%

Table 2: Performance comparison of super-fitting and defensive distillation (DD)

Model		Clean	FGSM	BIM-20
MiddleCNN	DD	86.79%	82.31%	82.21%
	Ours	89.05%	89.05%	89.05%
ResNet-18	DD	80.98%	78.40%	78.35%
	Ours	83.87%	83.87%	83.87%

where,

$$s = \operatorname{argmax} z_i \text{ and } s \neq y$$

In Eq. (17), z_s is the maximum value of prediction scores other than the true label (i.e., class scores that are not related to the true label). In fact, the goal of minimizing the scores of all irrelevant classes can be achieved just by minimizing z_s .

Table 1 shows the effect of MUCS and the CE loss on the super-fitting state of CIFAR-10, including the convergence speed and the final robustness accuracy (against PGD-20).

The experimental parameter settings in Table 1 are consistent with those in Fig. 1. The experimental results show that compared with the CE loss, although the accuracy of MUCS on the original examples (Clean Accuracy) is reduced, its adversarial robustness (accuracy against adversarial attacks) is improved (Robustness Accuracy). Also, the number of iterations required to reach the super-fitting state is greatly reduced (Iterations). Therefore, this paper combines the CE loss and MUCS in the subsequent experiments and uses Eq. (18) to optimize the model:

$$\operatorname{minimize} CE(z, y) + (z_s - z_y) \quad (18)$$

Eq. (18) can ensure that the number of iterations of model training is greatly reduced, and the accuracy of the original examples and the adversarial examples can reach a high level (i.e., the trade-off will be better).

4 Experiment

In this section, to demonstrate the effectiveness of the method proposed in this paper, super-fitting is compared with defensive distillation, which also uses gradient-based defense. This paper conducts extensive experiments to compare the adversarial robustness of 50 defense models on CIFAR-10 and the more difficult task CIFAR-100. There are 38 CIFAR-10 defense models and 12 CIFAR-100 defense models, and most of

these are from recent top conferences (e.g., ICML, NeurIPS, ICLR, ICCV, CVPR).

Setup. 1) In the comparison experiment of super-fitting and defensive distillation, this paper adopts the weak attack algorithms FGSM and BIM-20 for adversarial robustness evaluation; 2) To compare with state-of-the-art defense models, this paper adopts the more powerful PGD-100, APGD-100, and standard A^3 ; 3) The Adam optimizer is used for super-fitting training in all experiments, and the learning rate is $1e-3$. The hyperparameters of the attack algorithm are set as $\epsilon = 8.0/255$ and step size = $\epsilon/10$. The CE loss is used to calculate the gradient during the attack, and other parameters are kept at default.

Results. This paper shows the final experimental comparison results in Table 2 and Table 3. Table 2 shows that super-fitting performs better for the gradient-based defense methods. It is theoretically possible to make the gradient vanish completely. Table 3 shows that the model is robust against CE-based white-box adversarial attacks on the CIFAR-10 and CIFAR-100 datasets, and the super-fitting method performs better than other methods.

The experiments in Table 2 are performed on CIFAR-10, and two network architectures are taken for comparison (MiddleCNN and ResNet-18). The teacher network and student network model architectures used in defense distillation are consistent, and the distillation temperature is set to 100. The experimental results show that our proposed method works better than defensive distillation. Also, super-fitting can completely defend against weak attack algorithms like FGSM and BIM-20 (adversarial accuracy equal to the clean one).

This paper compares the performance of super-fitting with other recent excellent defense methods on the test sets of CIFAR-10 and CIFAR-100 datasets (1280 images are randomly selected, and the batch size is set to 128). Meanwhile,

Table 3: Performance of super-fitting against powerful attack

CIFAR-10 Defense Model		Clean	PGD	APGD	A ³
MiddleCNN(20.33MB)	super-fitting	87.32%	86.56%	84.33%	78.59%
ResNet-18(43.96MB)	Adv-regular [19]	88.99%	80.76%	68.03%	69.29%
	FBTF [23]	86.74%	69.41%	60.67%	47.26%
	CNL [26]‡	84.60%	71.25%	64.62%	76.71%
	Understanding FAST [27]	83.97%	66.19%	60.77%	47.34%
	Proxy [28]	84.01%	65.09%	60.49%	59.68%
	DNR [29]	84.35%	62.12%	58.03%	45.62%
WRN-28-4(48.95MB)	OAT [30]	83.95%	61.44%	57.78%	57.34%
WRN-28-4(48.95MB)	MMA [31]	87.08%	61.89%	60.71%	52.03%
ResNet-50(95.66MB)	Robustness [32]	87.06%	61.67%	60.50%	52.57%
WRN-28-10(205.17MB)	MART [33]†	84.35%	61.32%	57.99%	61.01%
	Feature-scatter [34]	84.92%	62.29%	58.69%	72.34%
	Adv-inter [35]	85.51%	63.51%	60.06%	75.23%
	AWP [36]†	85.86%	63.69%	60.51%	65.39%
	Geometry [37]†‡	86.15%	63.96%	60.89%	67.81%
	Hydra [38]†	86.28%	63.50%	60.61%	58.98%
	Pre-train [39]	86.32%	63.12%	60.39%	57.65%
	Rst [40]†	86.54%	63.13%	60.53%	63.51%
	ULAT [41]†	86.71%	63.32%	60.86%	67.42%
	Fix-data [42]	86.80%	63.53%	61.21%	66.48%
WRN-34-10(257.42MB)	RLPE [43]†	87.03%	63.60%	61.38%	65.23%
	TRADES [18]‡	86.95%	63.25%	61.13%	57.57%
	AWP [36]	86.95%	63.17%	61.15%	60.85%
	Proxy [28]†	86.92%	63.09%	61.15%	61.48%
	Self-adaptive [44]‡	86.74%	62.80%	60.93%	56.71%
	Sensible [45]	86.96%	62.67%	60.74%	62.26%
	YOPO [22]	86.94%	62.03%	60.17%	46.09%
	IAR/SAT [46]	86.92%	61.72%	59.90%	53.82%
	LBGAT [47]‡	86.94%	61.37%	59.60%	54.84%
	FAT [21]	86.90%	61.25%	59.54%	57.42%
WRN-34-15(517.84MB)	OAT [30]	86.85%	61.41%	59.74%	65.07%
WRN-34-15(517.84MB)	RLPE [43]†	87.02%	61.67%	60.52%	61.25%
WRN-34-20(866.20MB)	Hyper-embe [48]	86.81%	61.44%	59.79%	63.12%
	Overfit [49]	86.75%	61.34%	59.74%	58.67%
	ULAT [41]	86.71%	61.25%	59.68%	58.75%
	LBGAT [47]‡	86.80%	61.09%	59.56%	58.12%
WRN-70-16(1294.64MB)	ULAT [41]	87.15%	61.84%	60.56%	60.46%
	ULAT [41]†	87.30%	61.84%	60.42%	67.96%
	Fix-data [42]	87.16%	62.17%	60.98%	67.03%
CIFAR-100 Defense Model		Clean	PGD	APGD	A ³
MiddleCNN(20.68MB)	super-fitting	59.21%	55.19%	52.32%	41.71%
ResNet-18(44.14MB)	Overfit [49]	55.16%	37.95%	36.30%	20.46%
	OAT [30]	57.06%	36.04%	34.78%	32.96%
WRN-28-10(205.39MB)	Pre-train [39]	58.32%	36.07%	35.03%	35.85%
	Fix-data [42]	59.13%	36.27%	35.37%	37.73%
WRN-34-10(257.64MB)	AWP [36]	59.23%	36.21%	35.42%	35.54%
	IAR/SAT [46]	59.65%	34.69%	33.86%	26.40%
	LBGAT [47]‡	59.86%	34.76%	34.01%	36.56%
	OAT [30]	60.27%	34.78%	34.05%	34.68%
WRN-34-20(866.64MB)	LBGAT [47]‡	60.47%	34.81%	34.07%	35.23%
WRN-70-16(1295.00MB)	ULAT [41]	60.44%	34.12%	33.54%	32.50%
	ULAT [41]†	62.61%	35.63%	35.16%	40.00%
	Fix-data [42]	62.93%	36.27%	35.81%	39.53%

this paper uses the original examples, the adversarial examples generated by PGD-100, APGD-100, and the default version of A^3 in nine network model architectures (three basic architectures of MiddleCNN, ResNet, Wide ResNet/WRN [4]) to evaluate the adversarial robustness of the models. The results are shown in Table 3, where the first column presents the defense methods, network architectures, and model parameters (the one marked with ‡ denotes that $\epsilon = 0.031$, and the models marked with † denote that they use an additional unlabeled dataset in the training phase). “Clean” presents the accuracy of the model under the original examples; PGD, APGD, and A^3 respectively present the accuracy of the models under adversarial examples generated by PGD-100, APGD-100, and the default version of A^3 algorithms. Obviously, the super-fitting method proposed in this paper can obtain higher adversarial robustness with smaller models (i.e., fewer parameters).

5 Conclusion

This paper first introduces the super-fitting state in the model training process. In this state, the accuracy of a trained model under clean examples will decrease slightly, but its adversarial robustness will be greatly improved. Then, this paper analyzes the mathematical reasons that lead to the super-fitting phenomenon and theoretically proves that under the floating-point operation of the modern computer, super-fitting can perfectly handle CE-based white-box adversarial attacks (even future ones). Finally, for the problem that super-fitting requires a lot of iterative training, this paper proposes an optimization strategy called MUCS, which greatly reduces the number of iterations required for the model to reach the super-fitting state. Compared with about 50 recent defense models, the proposed defense method performs the best against CE-based white-box adversarial attacks.

References

1. He, K., et al. Deep residual learning for image recognition. in Proceedings of the IEEE conference on computer vision and pattern recognition. 2016.
2. Huang, G., et al. Densely connected convolutional networks. in Proceedings of the IEEE conference on computer vision and pattern recognition. 2017.
3. Szegedy, C., et al. Rethinking the inception architecture for computer vision. in Proceedings of the IEEE conference on computer vision and pattern recognition. 2016.
4. Zagoruyko, S. and N. Komodakis, Wide residual networks. arXiv preprint arXiv:1605.07146, 2016.
5. Gu, S. and L. Rigazio, Towards deep neural network architectures robust to adversarial examples. arXiv preprint arXiv:1412.5068, 2014.
6. Osadchy, M., et al., No bot expects the DeepCAPTCHA! Introducing immutable adversarial examples, with applications to CAPTCHA generation. IEEE Transactions on Information Forensics and Security, 2017. 12(11): p. 2640-2653.
7. Papernot, N., et al. Distillation as a defense to adversarial perturbations against deep neural networks. in 2016 IEEE symposium on security and privacy (SP). 2016. IEEE.
8. Madry, A., et al., Towards deep learning models resistant to adversarial attacks. arXiv preprint arXiv:1706.06083, 2017.
9. Szegedy, C., et al., Intriguing properties of neural networks. arXiv preprint arXiv:1312.6199, 2013.
10. Croce, F. and M. Hein. Reliable evaluation of adversarial robustness with an ensemble of diverse parameter-free attacks. in International conference on machine learning. 2020. PMLR.
11. Carlini, N. and D. Wagner, Towards Evaluating the Robustness of Neural Networks, in 2017 IEEE Symposium on Security and Privacy (SP). 2017. p. 39-57.
12. Goodfellow, I.J., J. Shlens, and C. Szegedy, Explaining and harnessing adversarial examples. arXiv preprint arXiv:1412.6572, 2014.
13. Kurakin, A., I. Goodfellow, and S. Bengio, Adversarial examples in the physical world. 2016.
14. Moosavi-Dezfooli, S.-M., A. Fawzi, and P. Frossard. Deepfool: a simple and accurate method to fool deep neural networks. in Proceedings of the IEEE conference on computer vision and pattern recognition. 2016.
15. Tashiro, Y., Y. Song, and S. Ermon, Diversity can be transferred: Output diversification for white-and black-box attacks. Advances in Neural Information Processing Systems, 2020. 33: p. 4536-4548.
16. Liu, Y., et al., Practical evaluation of adversarial robustness via adaptive auto attack. arXiv preprint arXiv:2203.05154, 2022.
17. Athalye, A., N. Carlini, and D. Wagner. Obfuscated gradients give a false sense of security: Circumventing defenses to adversarial examples. in International conference on machine learning. 2018. PMLR.
18. Zhang, H., et al. Theoretically principled trade-off between robustness and accuracy. in International Conference on Machine Learning. 2019. PMLR.
19. Jin, C. and M. Rinard, Manifold regularization for adversarial robustness. arXiv preprint arXiv:2003.04286, 2020. 1.
20. Cai, Q.-Z., et al., Curriculum adversarial training. arXiv preprint arXiv:1805.04807, 2018.
21. Zhang, J., et al. Attacks which do not kill training make adversarial learning stronger. in International Conference on Machine Learning. 2020. PMLR.
22. Zhang, D., et al., You only propagate once: Accelerating adversarial training via maximal principle. arXiv preprint arXiv:1905.00877, 2019.
23. Wong, E., L. Rice, and J.Z. Kolter, Fast is better than free: Revisiting adversarial training. arXiv preprint arXiv:2001.03994, 2020.

24. Ioffe, S. and C. Szegedy. Batch normalization: Accelerating deep network training by reducing internal covariate shift. in International conference on machine learning. 2015. PMLR.
25. Kingma, D.P. and J. Ba. Adam: A method for stochastic optimization. arXiv preprint arXiv:1412.6980, 2014.
26. Atzmon, M., et al., Controlling neural level sets. Advances in Neural Information Processing Systems, 2019. 32.
27. Andriushchenko, M. and N. Flammarion, Understanding and improving fast adversarial training. Advances in Neural Information Processing Systems, 2020. 33: p. 16048-16059.
28. Schwag, V., et al., Improving adversarial robustness using proxy distributions. arXiv preprint arXiv:2104.09425, 2021.
29. Kundu, S., et al. DNR: A tunable robust pruning framework through dynamic network rewiring of DNNs. in Proceedings of the 26th Asia and South Pacific Design Automation Conference. 2021.
30. Addepalli, S., et al., Towards Achieving Adversarial Robustness Beyond Perceptual Limits. 2021.
31. Ding, G.W., et al., Mma training: Direct input space margin maximization through adversarial training. arXiv preprint arXiv:1812.02637, 2018.
32. Engstrom, L., et al., Robustness (python library). 2019.
33. Wang, Y., et al. Improving adversarial robustness requires revisiting misclassified examples. in International Conference on Learning Representations. 2019.
34. Zhang, H. and J. Wang, Defense against adversarial attacks using feature scattering-based adversarial training. Advances in Neural Information Processing Systems, 2019. 32.
35. Zhang, H. and W. Xu, Adversarial interpolation training: A simple approach for improving model robustness. 2019.
36. Wu, D., S.-T. Xia, and Y. Wang, Adversarial weight perturbation helps robust generalization. Advances in Neural Information Processing Systems, 2020. 33: p. 2958-2969.
37. Zhang, J., et al., Geometry-aware instance-reweighted adversarial training. arXiv preprint arXiv:2010.01736, 2020.
38. Schwag, V., et al., Hydra: Pruning adversarially robust neural networks. Advances in Neural Information Processing Systems, 2020. 33: p. 19655-19666.
39. Hendrycks, D., K. Lee, and M. Mazeika. Using pre-training can improve model robustness and uncertainty. in International Conference on Machine Learning. 2019. PMLR.
40. Carmon, Y., et al., Unlabeled data improves adversarial robustness. Advances in Neural Information Processing Systems, 2019. 32.
41. Gowal, S., et al., Uncovering the limits of adversarial training against norm-bounded adversarial examples. arXiv preprint arXiv:2010.03593, 2020.
42. Rebuffi, S.-A., et al., Fixing data augmentation to improve adversarial robustness. arXiv preprint arXiv:2103.01946, 2021.
43. Sridhar, K., et al., Robust Learning via Persistency of Excitation. 2021.
44. Huang, L., C. Zhang, and H. Zhang, Self-adaptive training: beyond empirical risk minimization. Advances in neural information processing systems, 2020. 33: p. 19365-19376.
45. Kim, J. and X. Wang, Sensible adversarial learning. 2019.
46. Sitawarin, C., S. Chakraborty, and D. Wagner, Improving adversarial robustness through progressive hardening. 2020.
47. Cui, J., et al., Learnable Boundary Guided Adversarial Training. 2020.
48. Pang, T., et al., Boosting Adversarial Training with Hypersphere Embedding. 2020.
49. Rice, L., E. Wong, and Z. Kolter. Overfitting in adversarially robust deep learning. in International Conference on Machine Learning. 2020. PMLR.